Demonstration of Classification Task Using Optical Neural Network Based on Si Microring Resonator Crossbar Array

Shuhei Ohno[(1)], Kasidit Toprasertpong [(1)], Shinichi Takagi[(1)], Mitsuru Takenaka[(1)]

[(1)] Department of Electrical Engineering and Information Systems, The University of Tokyo, Japan
ohno@mosfet.t.u-tokyo.ac.jp

Abstract *We demonstrate Si microring resonator crossbar array as a programmable nanophotonic processor. By using multi-wavelength optical signal and monolithically integrated Ge photodetectors, we performed multiply-accumulate operation for optical neural network. We demonstrated classification task for Iris dataset, resulting in prediction accuracy of 91%.*

Introduction

Deep learning, a mathematical model based on neural network that is inspired by human brain, is one of the technologies that has been widely used in various fields such as image recognition, speech recognition, translation, medical research, automatic driving, and so on. Deep learning includes a lot of multiply-accumulate (MAC) operations, which need numerous computation time and power consumption for conventional computing technology. On the other hand, the current electrical computing faces the fundamental scaling limit since Moore's law is approaching to its end[1]. Therefore, novel computing architectures based on optical neural network (ONN), which potentially enables high computational efficiency and low latency without Moore's law, has been proposed. Especially, owing to the rapid growth of a CMOS-compatible silicon photonics platform, ONN featuring Si programmable nanophotonic processor (PNP) has attracted a lot of attention as a deep learning accelerator. To perform the MAC operation in the optical domain, an optical interference unit (OIU) based on meshed Mach-Zehnder interferometers (MZI)[3] and a weight bank based on cascaded microring resonator (MRR)[4]-[6] have been investigated. An OIU enables arbitrary linear transformation in optical domain, while the size of a MZI may restrict the scalability of a PNP. Also, despite of small dimension of an MRR, a weight bank has inner loops that cause resonator-like feedback[5], hindering its scalability.

To solve these issues, we have proposed a PNP based on MRR crossbar array for ONN, as shown in Fig. 1[7]. This PNP works by injecting multi-wavelength optical signal as an input vector $\boldsymbol{x}$. Each add-drop MRR with an optical phase shifter works as a programmable multiplier for each input wavelength where a dropped optical power at each wavelength can be tuned by a phase shifter. An integrated photodetector (PD) works as an adder by converting multiple optical signals into an electrical signal simultaneously. Since the proposed crossbar array configuration does not cause a resonator-like feedback, the MRR crossbar array can realize a large-scale PNP.

In the previous work, we demonstrated most primitive MAC operation using test element devices consisting of two MRRs[7]. In this paper, we prototyped a fully integrated Si MRR crossbar array with Ge PDs. We successfully achieved MAC operation and implement ONN for classification task.

Prototype chip

To demonstrate ONN, we designed an MRR crossbar array as a prototype chip based on Si photonics platform. Figure 2(a) shows a plan-view photograph of the fabricated 3×3 Si MRR crossbar array with 3 Ge PDs, enabling 3×3 matrix operation. The height and width of Si strip waveguides were 200 nm and 400 nm, respectively. At the input ports, which correspond to Port 1-3 in Fig. 1, spot size converters (SSCs) were integrated to reduce the coupling loss from a lensed fiber to the Si waveguide. Figure 2(b) shows an MRR, a waveguide crossing, and a TiN heater implemented in the MRR crossbar array. The radius and gap of MRRs were designed to be 10 μm and 200 nm, respectively. To reduce diffraction loss and crosstalk, a waveguide crossing consisting of four ellipses[8] was

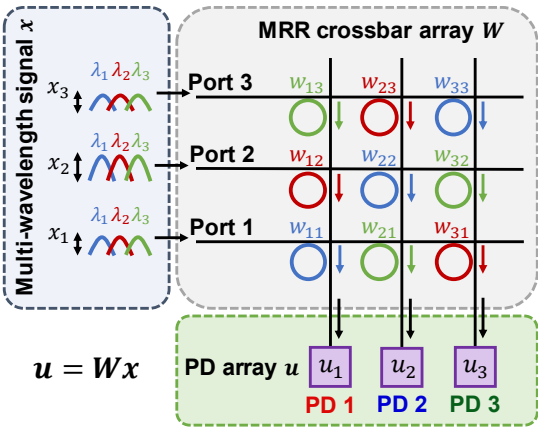

Fig. 1: Schematic of MRR crossbar array.

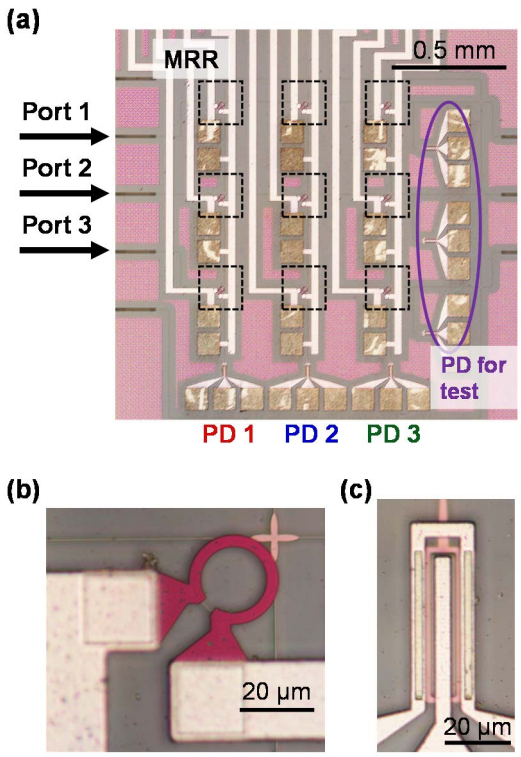

Fig. 2: (a) Microscope image of MRR crossbar array, (b) MRR with TiN heater, and (c) Ge PD.

employed. The TiN heater works as optical phase shifter driven by the thermo-optic effect in Si. At the output ports, Ge PDs[9] shown in Fig. 2(c) were integrated to convert the output optical signal to electrical current. The prototype chip was mounted on a printed circuit board (PCB) with wire bonding.

We evaluated the properties of the components of the MRR crossbar array. Figure 3(a) shows output spectra of single MRR when a voltage applied to the phase shifter was swept from 0 V to 1 V. Owing to the thermo-optic effect, we obtained a sufficient phase shift for tuning the resonance wavelength of the MRR whose free spectrum range was 8.7 nm. When applied voltage was 1 V, quality factor (Q factor) of the MRR was about 6700. Figure 3(b) shows I-V characteristics of a Ge PD shown in the purple eclipse of Fig. 2(a) with and without optical input at a 1550 nm wavelength. At -1 V bias voltage, the dark current and photocurrent when the power of optical input was 3 dBm were 200 nA and 12.6 μA, respectively. The estimated intrinsic responsivity of the PD was 0.66 A/W. These MRR and PD are applicable for following demonstration of 3×3 matrix operation.

Measurement setup

Figure 4 shows an experimental setup for the demonstration of an ONN using the MRR crossbar array. Multiple tunable laser diodes (TLDs) and a multiplexer (MUX) consisting of

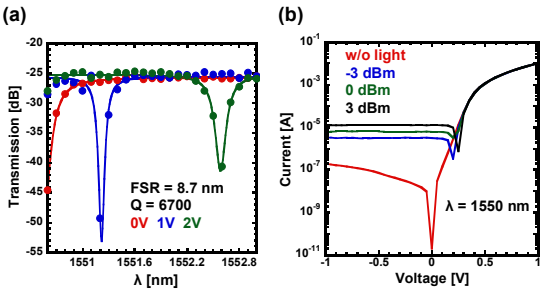

Fig. 3: Characteristics of (a) MRR and (b) Ge PD in the MRR crossbar array.

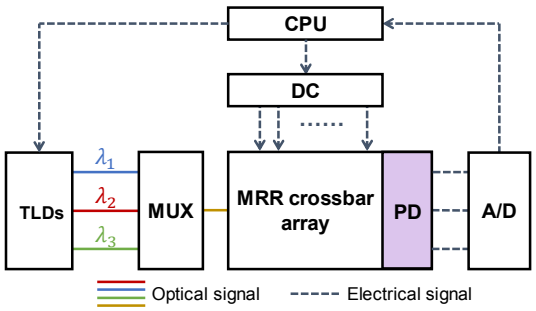

Fig. 4: Experimental setup for demonstration of optical neural network using MRR crossbar array.

cascaded 3 dB couplers were used to generate multi-wavelength optical signals at wavelengths λ_1, λ_2, and λ_3 shown in Fig. 1. A lensed fiber was used to inject the optical signal to each input ports in the MRR crossbar array. Photocurrents from the Ge PDs were received using analog-to-digital converters (A/Ds). All phase shifters were electrically controlled by a multi-output direct current (DC) source. A personal computer with a 64-bit CPU was used to control applied voltage on the phase shifters and to read out the output currents of the PD.

Calibration of MRR crossbar array

At first, by injecting single-wavelength optical signal, we calibrated each phase shifter of the MRR so that each assigned wavelength will be dropped as shown in Fig. 1. Figure 5(a) shows the calibrated dropped spectra of nine MRRs measured by the Ge PD at the three output ports. Since all resonance peaks of the MRR did not overlap each other, matrix elements w_{ij} can be programmed independently to perform MAC operation by applying additional voltage to the phase shifter of the MRRs.

To suppress the impact of the thermal crosstalk between MRRs during setting matrix elements w_{ij}, we applied the feedback control to the phase shifters by monitoring the photocurrent of the Ge PDs[6] so that the difference between the target photocurrent and monitored photocurrent was minimized. This feedback control was repeated about 50 times for all phase shifters. Figure 5(b) shows outputs of the MRR crossbar array after

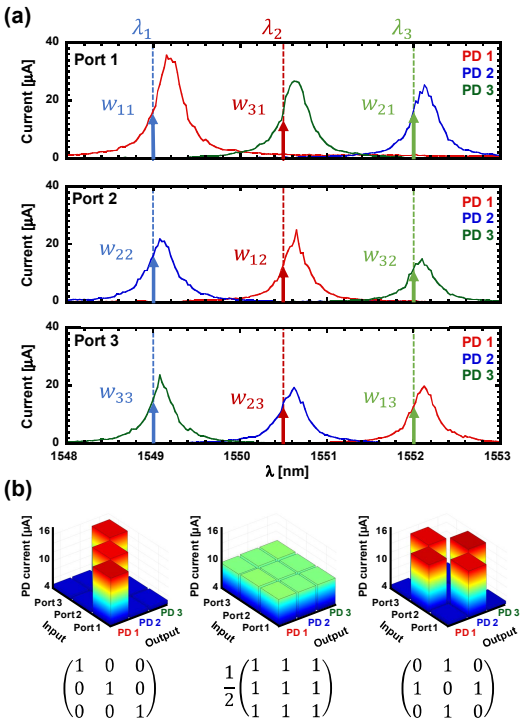

Fig. 5: (a) Dropped spectra of the nine MRRs measured by integrated Ge PDs after calibration. and (b) output of MRR crossbar array exhibiting three representative 3×3 matrices.

the optimization of the control of the phase shifter, exhibiting three representative 3×3 matrices where 1 and 0 states in the matrix elements were expressed by 15 μA and 5 μA, respectively. Owing to the feedback calibration, arbitrary matrices could be expressed even with the existence of the thermal crosstalk, showing the feasibility of application of MRR crossbar array for ONN.

Demonstration of ONN

We implemented an ONN, including a three-dimension hidden layer shown in Fig. 6(a), by using the MRR crossbar array as a PNP and demonstrated three-specie Iris flower classification using Iris flower dataset[10]. "Sepal length," "Petal width," and "Petal length" of the dataset were used as attributes of the ONN. The ReLU function was employed as the an activation function. Figure 6(b) shows a schematic of the demonstration flow. As shown in Fig. 6(b), MAC operation was performed by deviding the matrix elements into plus and minus values. The final result of MAC operation was obtained by subtraction of the plus and minus values.

To deterimine the weights in the ONN shown in Fig. 6(a), we performed training of the ONN model on a computer based on a back propagation algolithm using 50 instances in the dataset. Next, we programmed the MRR crossbar array to perform MAC operation using the trained model. Finally, we evaluated the ONN

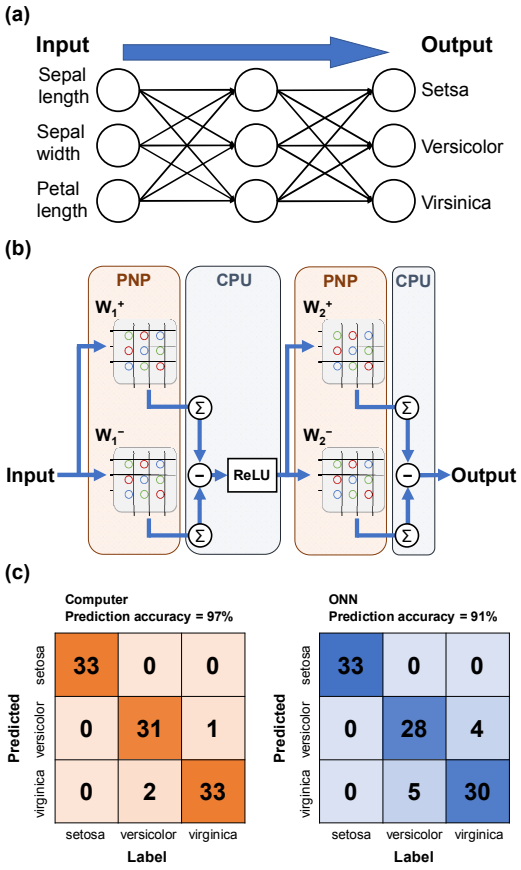

Fig. 6: (a) Schematic of ONN for demonstration and (b) experiment setup for implementing ONN, and (c) label prediction results of conventional computer (left) and ONN (right).

using the MRR crossbar array by testing classification of 100 instances which were not used in the training. Figure 6(c) shows results of the classification task. The implemented ONN correctly identified 91/100 instances, while a conventional computer identifies 97/100 instances. This result showed the feasibility of the ONN using the MRR crossbar array. We attributed the error of the ONN to the fluctuation in coupling between the lensed fiber and Si waveguide during the inference, which can be reduced by improving the measurement system.

Conclusions

We have prototyped the 3×3 MRR crossbar array and successfully demonstrated MAC operation. Using the MRR crossbar array, we have successfully implemented ONN for classification task, resulting in prediction accuracy of 91%. Therefore, the MRR crossbar array is promising as a PNP.

Acknowledgements

This work was partly supported by JST CREST Grant Number JPMJCR1907 and the Asahi Glass Foundation.

References

[1] K. Kitayama *et al.*, “Novel frontier of photonics for data processing—Photonic accelerator”, APL Photon., vol. 4, pp. 090901, 2019.

[2] L. D. Marinis *et al.*, “Photonic Neural Networks: A Survey”, IEEE Access, vol. 7. pp. 175827–175841, 2019.

[3] Y. Shen *et al.*, “Deep learning with coherent nanophotonic circuits”, Nat. Photonics, vol. 11, pp. 441–446, 2017.

[4] A. N. Tait *et al.*, “Neuromorphic photonic networks using silicon photonic weight banks”, Sci. Rep., vol. 7, vol. 7430, pp. 8, 2017.

[5] A. N. Tait *et al.*, “Microring Weight Banks”, IEEE J. Sel. Top. Quantum Electronics, vol. 22, no. 6, 2016.

[6] C. Huang *et al.*, “Demonstration of scalable microring weight bank control for large-scale photonic integrated circuits”, APL Photon., vol. 5, pp. 040803, 2020.

[7] S. Ohno *et al.*, “Si microring resonator crossbar arrays for deep learning accelerator”, Jpn. J. Appl. Phys., vol. 59, no. SGGE04, 2020.

[8] F. Shinobu *et al.*, “Low-loss simple waveguide intersection in silicon photonics”, Electro. Lett., vol. 46, pp. 1149, 2010.

[9] J. Wang *et al.*, “Ge-Photodetectors for Si-Based Optoelectronic Integration”, Sensors, vol. 11, pp. 696–718, 2011.

[10] https://archive.ics.uci.edu/ml/datasets/iris